IEEE Access
Multidisciplinary | Rapid Review | Open Access Journal

Received December 5, 2020, accepted December 27, 2020, date of publication January 8, 2021, date of current version January 19, 2021.

Digital Object Identifier 10.1109/ACCESS.2021.3050005

Combined Trajectory Planning and Tracking for Autonomous Vehicle Considering Driving Styles

HAORAN LI[1,2], (Student Member, IEEE), CHAOZHONG WU[1,2], DUANFENG CHU[1,2], (Member, IEEE), LIPING LU[3], AND KEN CHENG[3]

[1]Intelligent Transportation Systems Research Center, Wuhan University of Technology, Wuhan 430063, China
[2]School of Automotive Engineering, Wuhan University of Technology, Wuhan 430063, China
[3]School of Computer Science and Technology, Wuhan University of Technology, Wuhan 430070, China

Corresponding author: Duanfeng Chu (chudf@whut.edu.cn)

This work was supported in part by the National Key Research and Development Program of China under Grant 2018YFB1600600; in part by the National Natural Science Foundation of China under Grant 51675390, Grant 51775396, and Grant U1764262; and in part by the Hubei Province Innovation Group Project under Grant 2017CFA008.

ABSTRACT Autonomous driving is one of the promising technologies to tackle traffic accident and congestion problems nowadays. Even though an autonomous vehicle is operated without humans, it is necessary to reflect the driving characteristics of a human driver. This can increase user acceptance to autonomous driving system, which in turn will improve driving safety because of human occupants' trust in it. In this paper, a combined trajectory planning and tracking algorithm is proposed for the vehicle control. Firstly, traffic environments and driving styles are modeled with the Artificial Potential Field (APF) approach. Secondly, those APF values are integrated into the Model Predictive Control (MPC) design process, which can optimize the trajectories and control outputs. In this way, we add people's driving habits and styles into the controller, so that the controlled vehicle can move under the effects of the traffic environments and human's driving styles. At last, autonomous driving, which reflects two types of human drivers' driving styles (a cautious driving style and an aggressive one), is tested by the simulation experiments in two scenarios (car-following and lane-changing). Furthermore, the result demonstrates that the proposed algorithm can reflect driving styles. Accordingly, this novel controller can be utilized in the autonomous vehicle control field.

INDEX TERMS Autonomous vehicle, artificial potential field, driving style, MPC, trajectory planning and tracking.

I. INTRODUCTION

Autonomous driving is the current research hotspot, which mainly includes trajectory planning and trajectory tracking [1]. Specifically, the trajectory planning of autonomous driving is to design a trajectory suitable for driving environments. Besides, the trajectory tracking is the part to execute the autonomous driving which ensures that the vehicle follows the planned trajectory. Given that the first principle of autonomous driving is safety, the trajectory planning and trajectory parts should be capable of bypassing the obstacles and moving within the road boundaries.

The associate editor coordinating the review of this manuscript and approving it for publication was Xiangxue Li.

In order to achieve user acceptance, we should have the autonomous vehicles which are not only safe and reliable but also comfortable in terms of user experience. However, the individual perception of comfort may vary considerably among various vehicle users. For example, some users might prefer sporty driving with high accelerations, while others might prefer a soft style. Typically, a human driver's style is characterized by a large number of parameters representing acceleration profiles, distances to surrounding vehicles, speed during lane-changing, etc. [2]

A. PERSONALIZED DRIVER MODELS

In fact, driving behaviors vary greatly among different human drivers according to their genders, ages, driving experience,

driving habits, etc. [3]. Many researches have been carried out on driving styles and individual driving. [4]– [6]. Furthermore, the corresponding driving trajectories can be planned according to different types of his/her driving style. Subsequently, the autonomous vehicle users can switch to their own preferred mode to improve driving comfort [7].

In recent years, some researches have been conducted on autonomous vehicles in which driving styles are considered. Specifically, Kuderer *et al.* [2]. propose a research from demonstration approach to learn the model parameters for each user from their observed driving styles. They propose a feature-based inverse reinforcement learning (IRL) method to learn driving styles from demonstrations. In this case, features are mappings from trajectories to real values which capture important properties of driving styles. In addition, they have shown that their approach is capable of learning cost functions and reproducing different driving styles using data from real drivers. Lefèvre *et al.* [8] present a learning-based framework for the autonomous driving which combines a driver model and a predictive controller. In this situation, the learning-based driver model can generate commands resembling those of a human driver. Moreover, the commands generated by the driver model are utilized as a reference by an MPC controller, which is in charge of guaranteeing safety. Finally, they implement and test the proposed framework for the longitudinal control of an autonomous vehicle. Hasenjager *et al.* [9] review personalization approaches for ADAS systems that can be adopted according to the drivers' preferences, driving styles, skills and driving patterns. Xing *et al.* design a personalized joint time series modeling system based on deep learning method to jointly estimate the future energy consumption index and predict leading vehicle trajectories considering different driving styles [10], [11]. However, the above method requires a large amount of data, and the implementation cost is high. In the light of this fact, the changing of the learning model will be difficult once it is built completely. Compared with the methods above, the method proposed in this paper only needs to set the parameters of the APF in advance, which has a lower cost and can be changed at any time according to the needs of different individuals.

B. AUTONOMOUS VEHICLE BASED ON APF AND MPC

Actually, advanced trajectory planning methods for autonomous vehicles include APF approach, random search method, and other intelligent algorithm-based methods, such as the neural network algorithm, the genetic algorithm, and the swarm intelligence algorithm, etc. In this case, the APF approach is one of the most attractive trajectory planning methods because of its simple structure, clear mathematical description, and good real-time performance. The APF is firstly applied in trajectory planning of mobile robots [12], and it can generate a path for a vehicle to reach the target point without any collisions by assigning reasonable potential field functions for obstacles. Similarly, Huang *et al.* [13] present a novel motion planning and tracking framework for automated vehicles based on the APF elaborated a resistance approach. In addition, Wang *et al.* [14] present an obstacle avoidance path planning method for autonomous driving vehicles, and they study the path planning mechanisms of human drivers and demonstrate a safety APF model. These trajectory planning methods based on the APF all meet the safety requirements, but none of them consider various driving styles of human drivers.

MPC method is one of the most effective methods in trajectory tracking. Specifically, it can transform the vehicle tracking control into a limited time domain and constrained optimization problem. In addition, the MPC method is widely used in trajectory tracking of autonomous vehicles because of its ability to deal with constrained control problems. Guo *et al.* [15] propose an implementation scheme for an MPC path following controller, which considers the feasible road region and vehicle shape. Zhang *et al.* [16] integrate trajectory planner and tracking controller for autonomous vehicles to implement the collision avoidance. Li *et al.* [17] propose an obstacle avoidance controller based on nonlinear MPC, which is designed in the autonomous vehicle navigation. Berntorp *et al.* [18] put forward a nonlinear MPC scheme that adapts a tire model in response to the estimated road surface. Velhal *et al.* [19] present an improved linear time varying MPC controller for automatic steering control of unmanned vehicles, which can execute trajectory following at high speed on the slippery roads. Du *et al.* [20] design a controller that can simultaneously control the steering and speed of unmanned vehicles based on nonlinear MPC. Besides, the genetic algorithm is utilized to speed up optimization solutions.

As a matter of fact, MPC controller can also be used for trajectory planning by adding penalty of obstacles into the cost function of the MPC. Abbas *et al.* [21] establish an obstacle avoidance function through adding the distance between the obstacle and the vehicle. Soloperto *et al.* [22] provide a novel robust collision avoidance approach based on a general tube-based MPC framework. Wang *et al.* [23] take vehicle shapes into consideration as a convex polygonal region and develop a convex quadratic programming MPC scheme for the real-time collision avoidance.

In fact, the trajectory planning and tracking for autonomous vehicles are generally divided into two independent units. To be specific, the local trajectory planner designs a suitable trajectory, and then the tracking controller follows the planned trajectory. In recent years, some researches have begun to integrate trajectory planning and tracking into a unified module. For example, Huang *et al.* [24] add APF functions to the cost function. Likewise, Rasekhipour *et al.* [25] also designed an APF-based MPC controller for autonomous vehicles. Huang *et al.* [26] show a control algorithm combining APF approach with MPC, and they use the optimizer of the MPC controller to replace the gradient-descending method in the conventional APF approach. However, they only ensured the driving safety and did not consider different driving styles.

It is noteworthy that different autonomous vehicle occupants actually prefer different driving styles according to their own preferences or driving habits. However, only the traffic safety and congestion issues are considered in the conventional autonomous driving systems, which makes it impossible for us to select different driving style modes reflecting the occupants' preferences. Those situations may cause an unacceptability issue with autonomous driving. In addition, its occupants' unacceptability may cause dangers once some emergency traffic scenarios occur [9].

C. CONTRIBUTIONS

This paper proposed trajectory planning and tracking algorithms of the autonomous vehicles conforming to various driving styles, and the scenarios of autonomous driving include car-following and lane-changing. In these scenarios, the driving styles consist of the cautious one and the aggressive one, which can be switched by the user. In this paper, the trajectory planning and tracking problem is transformed into a unified optimization problem based on the APF modeling of driving environments and driving styles. Additionally, the local trajectory determined by the APF can be selected with the optimization algorithm in the MPC controller by adding the APF values to the cost function. In this way, we can generate a reference trajectory reflecting human drivers' driving style. Compared the data-driven driver model (deep learning, inverse reinforcement learning, etc.), the model here combining model-based with data-driven is easy to be built (simple structures and not based on hug data). In addition, to some tents, it is physically explainable, which is difficult for most data-driven methods.

This paper is organized as follows: In Section 2, the car-following behavior and the lane-changing behavior are analyzed. In Section 3, the APF models, which include environment and driving style APF, are established. In Section 4, the trajectory planning and tracking methods considering driving styles are represented. In Section 5, the proposed method is evaluated under several typical traffic scenarios, and the results are presented and discussed. Finally, Section 6 wraps up the paper by concluding the major findings.

II. DRIVING BEHAVIOR ANALYSIS

Typical vehicle behaviors on highway roads mainly include free-flowing, car-following and lane-changing, and the latter two behaviors are more complex for trajectory planning and tracking. Taking this into account, we chose some indicators reflecting driving style by analyzing the differences of driving behaviors in car-following and lane-changing scenarios.

A. CAR-FOLLOWING BEHAVIOR ANALYSIS

In the car-following scenario on highways, the longitudinal acceleration can be chosen as an indicator for a driver's driving style. In the process of approaching the preceding vehicle, the local vehicle needs to decelerate, and the main difference among drivers is the vehicle speed changing. The reason is that drivers' perceptions of longitudinal acceleration vary greatly. In this case, Wang *et al.* [27] analyze the driving styles in car-following scenarios. To be specific, they select three feature variables extracted from the Safety Pilot Model Deployment (SPMD) database, which include the distance from leading car, longitudinal accelerations, etc. For aggressive driving, the acceleration ranges are $\leq -0.24m/s^2$ and $\geq 0.23m/s^2$.

Another indicator to reflect a driver's driving style is the Time Headway (THW), which means the time spent in the local vehicle driving from its front to the rear of the preceding vehicle. Wang et al [28] indicate that THW is a typical variable that describes the characteristics of a driver. Furthermore, Bing Zhu *et al.* [29] also analyze the differences of THW among different drivers, and the THW of aggressive and cautious drivers are 1.32 seconds and 2.14 seconds, respectively.

In summary, we choose the longitudinal acceleration and the THW as the behavioral indicators reflecting the driving style of the autonomous vehicle in the car-following scenario.

B. LANE-CHANGING BEHAVIOR ANALYSIS

Lane-changing behavior is the behavior of the vehicle driving from the current lane to the adjacent lane with considering driving intention, comfort, etc. [30]. In this case, once the driver decides to change lanes, he should determine whether or not to execute lane-changing immediately based on the current driving environment. In [31], it points out that the lane-changing behaviors come into two categories: mandatory lane-changing and arbitrary lane-changing. To be specific, mandatory lane-changing must be accomplished within a certain time. Moreover, arbitrary lane-changing is performed when the driver tending to complete the driving task quickly encounters a slower obstacle vehicle in front. In this situation, we focus on the latter one which is the main lane-changing behavior on freeways.

The influence of driving style on lane-changing behavior on highways is analyzed in [32]. Fairclough el al. find that during conducting overtaking maneuvers, conservative drivers prefer a higher THW (Mean = 1.76 s) than either the neutral drivers (Mean = 1.23 s) or the aggressive drivers (Mean = 1.15 s). Doshi el al. [33] analyze differences in measured time from lane-changing initiation to lane crossing (time-to-lane-crossing) for different driving styles in the simulator experiment. It shows a significant difference ($p < 0.05$) among the different groups. In the case of lane-changing, they study how long it takes the drivers to drive from the initiation of the maneuver to the point of lane crossing, and they have given a distribution of the ''time-to-lane-crossing'' as a function of the driving style. Actually, the mean lane-changing durations of aggressive and cautious drivers are 1.7s and 2.5s, respectively. In all, we chose two feature variables (THW, lane-changing durations) to reflect the driver's driving style in the lane-changing scenario.

III. THE DESIGN OF APF MODELING

The analysis above show differences between cautious and aggressive drivers. These differences are concerned with the

longitudinal acceleration and the time headway in the car-following behavior, as well as the lane-changing duration and the THW in the lane-changing behavior. Therefore, these indicators are utilized to quantify driving styles in the APF modeling,

The APF modeling includes environment and driving style APF. To be specific, the environment APF describes the interaction of the autonomous vehicle with its surrounding environment. On the other hand, the driving style APF is adopted to express the influence of various driving styles on the trajectory planning.

A. ENVIRONMENT APF

1) THE APF OF BOUNDARY LINES

The vehicle can only drive between boundary lines. Thus, such APF prevents the vehicle from leaving the highway by making the APF values stay within infinite boundaries. On each side of the highway, we employ the following used in robotics motion planning:

$$U_{road} = A_{road} / \left(y - y_{road,j}\right) \tag{1}$$

where A_{road} is a APF factor, and $y_{road,j}$ is the lateral position of the j_{th} highway boundary line.

2) THEPOTENTIAL OF LANE LINE

In fact, the potential of lane lines differs from that of boundary lines in that the former is utilized to guide the vehicle moving along them. This APF value decreases while the vehicle approaches the lane centerlines, so we employ a quadratic function as follows:

$$U_{lane} = A_{lane} \left(y - y_{lane}\right)^2 \tag{2}$$

where A_{lane} is a APF factor, and y_{lane} is the lateral position of the lane's centerline.

3) THE APF OF TARGET POINT

As the vehicle moves forward along the lane, its front direction should always be selected as its target. This APF can ensure that the local vehicle moves forward, so that the APF's front part decreases when the distance from a front targeting point to the local vehicle decreases. That is to say, the APF of a targeting point is proportional to this distance and should be non-negative. Therefore, we employ a simple first order function to describe this APF value:

$$U_{goal} = \kappa \left(x - x_{car}\right) \tag{3}$$

where κ is a coefficient of the target APF value, x is the longitudinal position of targeting point.

4) THE APF OF OBSTACLE VEHICLE

The method to establish the APF of an obstacle vehicle is similar to the study of Wolf, *et al.* [26], [34]. We firstly establish the APF along the longitudinal direction of the obstacle vehicle, and then its total APF is expended based on the longitudinal APF. The area of the obstacle's potential field is divided into three parts, which is shown in Fig. 1.

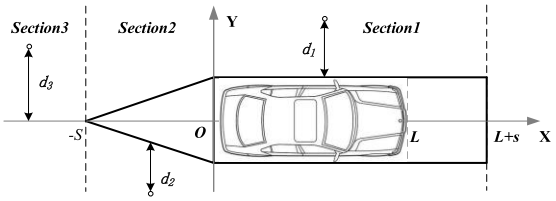

FIGURE 1. The potential description of the obstacle vehicle.

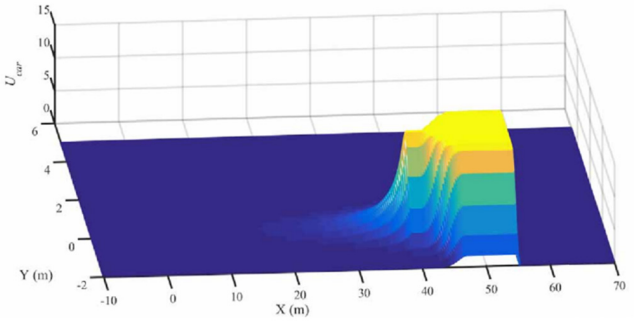

FIGURE 2. The APF of the obstacle vehicle.

At an arbitrary point p in any section, we want to calculate the APF value of the local vehicle, and the APF distribution rule is presented as follows:

$$A_{car} \begin{cases} U_{car}, & p \in Section1 \cup \in Section2 \\ v_r / \left(K - S\right), & p \in Section3 \cap v_r > 0 \\ 0, & p \in Section3 \cap v_r \leq 0 \end{cases} \tag{4}$$

where U_{car} is the maximum value of the APF, v_r denotes the relative speed between the local vehicle and the obstacle vehicle, and K denotes the longitudinal distance between the local vehicle and the obstacle vehicle. Besides, S denotes the safe distance, and it can be calculated as:

$$S = \phi \cdot V_r + S_{min} \tag{5}$$

where, ϕ is a scale coefficient, and S_{min} is the minimum safe distance.

A Gaussian-like function is adopted to model the lateral APF distribution illustrated in Equation (6).

$$A_{car_{all}} = A_{car} \exp\left(-d^2 / 2\sigma_{car}^2\right) \tag{6}$$

where A_{car} is the longitudinal APF value defined above, and d denotes the lateral distance from the local point to the nearest point on the obstacle vehicle. As shown in Fig. 1, if the point is in Area 1, then $d = d_1$; if the point is in Area 2, then $d = d_2$; if the point is in Area 3, then $d = d_3$. Additionally, σ_{car} represents the attenuation coefficient of the obstacle vehicle APF, and the APF of the obstacle vehicle is shown in Fig. 2.

All the APF values described above are combined to form a total environmental APF. The schematic diagram of the total environmental APF is shown in Fig. 3. We note that the Y-axis represents the road width, −1.5 to 1.5 represents the left lane, and 1.5 to 4.5 represents the right lane. Apart from this, the X-axis represents the position of the road in the longitudinal direction. The Z-axis represents the magnitude of the APF,

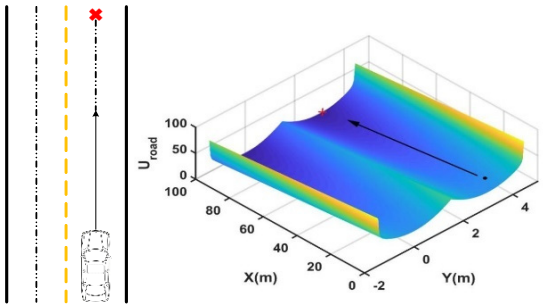

FIGURE 3. The APF of the traffic environment.

and the colder the color is, the lower the APF value is at that position. In addition, the Red Cross represents the lowest point of the APF on the right lane. The black point represents the current position of the local vehicle, and it will go to the lowest point of the APF along the direction of the arrow if there is no obstacle in front.

B. THE AP OF DRIVING STYLE

1) THE APF OF TIME HEADWAY

In the car-following mode, time headway APF ensures that the local vehicle maintains a certain safety distance to the front obstacle vehicle. This safety distance is determined according to the current driving mode the user select. Accordingly, we employ a quadratic function, as shown below.

$$U_{thw} = A_{thw}\left(THW_{cur} - THW_{exp}\right)^2 \tag{7}$$

where A_{thw} is an APF factor, and THW_{cur} and THW_{exp} are current and expected time headway. In this case, time headway APF decreases when the current time headway approaches the expected value, so it can guide the local vehicle to follow its preceding vehicle with a desired time headway.

2) THE APF OF LANE-CHANGING DURATION

The APF of lane-changing Duration is defined as follows:

$$U_{time} = A_{time}\left(t - t_{exp}\right)^2 \tag{8}$$

where A_{time} is an APF factor, and t_{exp} is the desired lane-changing duration of different driving styles. The APF of lane-changing duration guides the vehicle to complete the lane-changing within the desired time. In order to facilitate the programming of the algorithm, the lane-changing duration is converted into longitudinal distance in the lane-changing process. Subsequently, the desired lane-changing time can be obtained by adjusting the APF coefficient of adjacent lanes. In the lane-changing scenario, the average lane-changing speed can be estimated based on current speed. Therefore, the longitudinal distance can be obtained by multiplying the lane-changing duration by the average speed.

IV. THE TRAJECTORY PLANNING AND TRACKING CONSIDERING DRIVING STYLES

This section presents a combined trajectory planning and tracking algorithm for autonomous vehicles. Actually driving

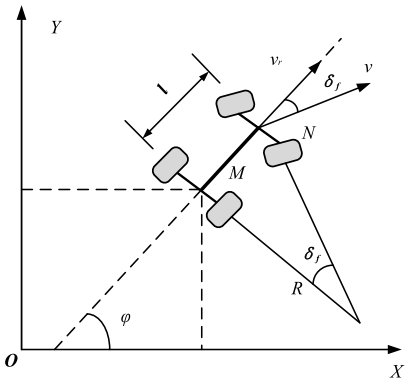

FIGURE 4. Vehicle kinematic model.

styles are taken into consideration in the method adopted in this method, which is different from other trajectory planning methods. The combined trajectory planning and tracking method is based on the MPC method, and the proposed APF for environment and driving style are added as parts of the objective function to avoid obstacle and reflect driving style simultaneously. The modeling methods under the car-following mode and the lane-changing mode are presented as follows.

A. CAR-FOLLOWING MODE

1) VEHICLE MODEL

The vehicle kinematics model is described in Fig. 4. Given the rear axle midpoint of the vehicle (x, y), the speed v is calculated as following.

$$v = \dot{x}\cos\varphi + \dot{y}\sin\varphi \tag{9}$$

where (x, y) stands for the vehicle position in the Cartesian coordinate, ϕ denotes the counterclockwise orientation of the vehicle from the x-axis, v denotes the speed, δ_f denotes the road front wheel steering angle. The vehicle kinematics model is illustrated below.

$$\chi = \begin{bmatrix} \dot{x} \\ \dot{y} \\ \dot{\varphi} \end{bmatrix} = \begin{bmatrix} \cos\varphi \\ \sin\varphi \\ \tan\delta_f / l \end{bmatrix} v \tag{10}$$

2) COSTFUNCTION

The cost function contains three parts. The first part is the APF U_{APF_follow}:

$$U_{APF\ follow} = U_{road} + U_{goal} + U_{thw} \tag{11}$$

where the environment APF U_{road} and U_{goal} are used to restrict the local vehicle to drive in the current lane, and the driving style APF U_{thw} is used to reflect the driving style.

The APF in the car-following scenario is shown in Fig.5, and the picture on the left is a schematic diagram of a car-following scenario. Additionally, the picture on the right shows the corresponding APF, and the X-axis represents the position of the road in the longitudinal direction. The Y-axis represents position of the road in lateral direction, in which $[-1.5, 1.5]$ is the right lane, and $[1.5, 4.5]$ is the left lane.

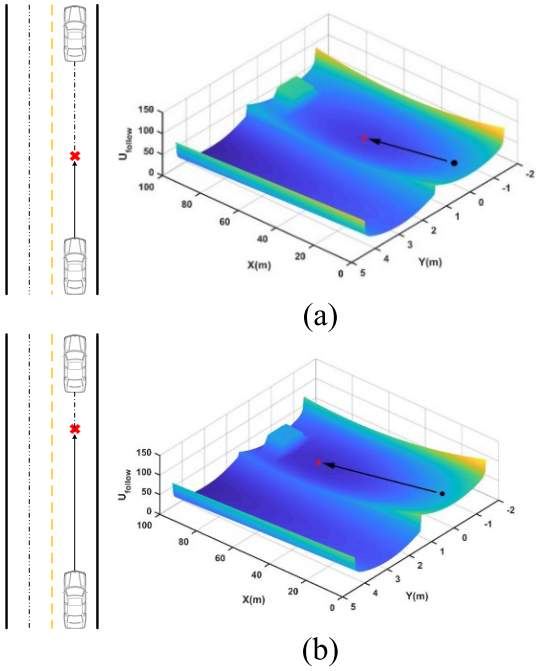

FIGURE 5. (a) Potential Field in the Car-Following Scenario (cautious) (b) Potential Field in the Car-Following Scenario (aggressive).

The bump in the right lane represents the obstacle car, which will generate a gravitational APF at a certain distance behind it, attracting the local car in a certain position behind it. Subsequently, the local car can maintain THW in a set value. In the APF diagram, the Red Cross represents the lowest point of the current APF and the local car will always go towards the position which has lower APF. Because of the existence of such a THW APF, the lowest point of the APF will always be kept at a fixed distance (THW$^*v_{car}$) from the car ahead. As shown below, Fig.5 (a) represents the cautious style, while Fig.5 (b) represents the aggressive style.

The second part of the cost function is speed tracking, and the last part is the control increment. Subsequently, the cost function is created in the following form.

$$\begin{aligned} J_{follow} &= (\xi(t), u(t-1), \Delta u(t)) \\ &= \sum_{i=1}^{N_p} \left\| U_{APF\ follow}(t+i\,|t) \right\|_Q^2 \\ &\quad + \sum_{i=1}^{N_p} \|v(t+i\,|t) - v_{des}\|_R^2 + \sum_{i=1}^{N_c} \|\Delta u(t+i\,|t)\|_S^2 \end{aligned} \tag{12}$$

where $u(t) = [v(t), \delta(t)]$ denotes the vehicle's control input vector at time t, $\Delta u(t)$ stands for the sequence of the future control increments, $U_{APF\_follow}(t+i\,|t)$ represents the APF value of the vehicle at time instant $t+i$, $v(t+i\,|t)$ represents the longitudinal velocity at time instant $t+i$, $\Delta u(t+i\,|t)$ represents the control increment at time instant $t+i$, N_p denotes the prediction horizon, N_c denotes the control horizon, v_{des} denotes the desire speed, and Q, R and S are weight matrix.

The cost function, i.e., Equation (12) includes three parts. Specifically, the first part is the APF value of the local vehicle, which is calculated by the vehicle kinematics model combined with APF function. The APF is introduced into the objective function to find those points with minimum potential field value as the optimal trajectory. In this case, the trajectory planning is mainly dependent on the APF, so the corresponding weights should be larger. The second part ensures that the local vehicle maintains the current desired speed. The third part is utilized to limit the control increment with the aim of preventing large change of control increment, so that the movement state of the vehicle can be changed gently and guarantee the comfort.

When we take into account the real driving conditions, the constraints are configured as follow:

$$\begin{aligned} 0 \le v &\le 1.1 * v_{des} \\ \dot{v}_{min} &\le \dot{v} \le \dot{v}_{max} \\ -25^\circ &\le \delta \le 25^\circ \\ -0.47^\circ/\mathrm{s} &\le \dot{\delta} \le 0.47^\circ/\mathrm{s} \end{aligned} \tag{13}$$

In summary, the optimal control problem of the trajectory planning considering driving style under car-following mode is:

$$\begin{aligned} &min_{\Delta u(t)} \ \left\{ J_{follow} = (\xi(t), u(t-1), \Delta u(t)) \right\} \\ &\text{s. t. } \xi(k+1) = f(\xi(k), u(k)) \\ &\quad u(k) = u(k+1) + \Delta u(k) \\ &\quad u_{min}(k) \le u(k) \le u_{max}(k) \\ &\quad \Delta u_{min}(k) \le \Delta u(k) \le \Delta u_{max}(k) \end{aligned} \tag{14}$$

The first element of the calculated control increment sequence is set as an input to the autonomous vehicle, and the next period continues the same optimization problem.

B. LANE-CHANGING MODE

The trajectory planning and tracking in the lane-changing mode is similar to the method in the car-following mode. The states of autonomous vehicles come into the free-flowing and lane-changing in the lane-changing mode. In the light of this fact, the logic in the lane-changing mode can be summarized as follows: selecting corresponding style for the lane-changing, and the local vehicle enters in the free running mode. When the triggering condition of lane-changing is reached, the vehicle begins to change lanes in the corresponding driving style. After the lane-changing process is completed, the vehicle returns to the free running mode.

The triggering condition of the lane-changing is the distance to the front vehicle, and the distance of different driving modes vary according to the analysis of Section ćò. If the driving mode is set as the cautious one, the local vehicle will begin to change lanes only when the triggering condition of cautious style is reached. In the free driving mode, the vehicle drives at the set speed and will not change lanes. Accordingly, the objective function of free-driving mode can be shown as

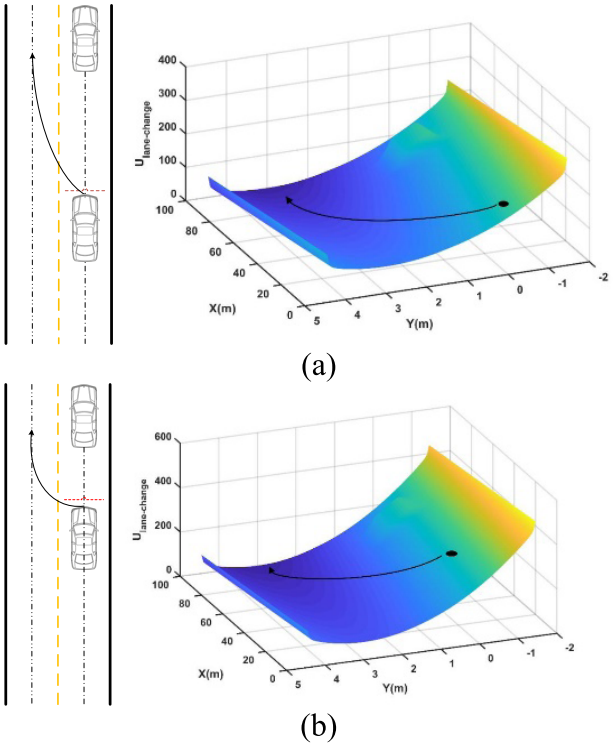

FIGURE 6. **(a) Potential field in the lane-change scenario when the lane-changing triggering condition is reached (cautious), (b) Potential field in the lane-changing scenario when the lane-changing triggering condition is reached (aggressive).**

below:

$$\begin{aligned} J_{free} &= (\xi(t), u(t-1), \Delta u(t)) \\ &= \sum_{i=1}^{N_p} \left|\left| U_{APFfree}(t+i|t) \right|\right|_{\mathrm{Q}}^2 \\ &\quad + \sum_{i=1}^{N_p} \| v(t+i|t) - v_{des} \|_R^2 + \sum_{i=1}^{N_c} \| \Delta u(t+i|t) \|_S^2 \end{aligned} \tag{15}$$

where U_{APF_free} is the sum of road potential, lane potential and target potential, as following.

$$U_{APF\ free} = U_{road} + U_{goal} + U_{lane} \tag{16}$$

U_{APF_free} only contains environmental APF, because driving style is not considered in the free-flowing mode. Vehicle APF is not included, and the other parts of the cost function are the same as Equation (12). The triggering condition is embedded in the free-flowing mode, and it will judge the THW with the threshold in each step. Once the triggering condition reached, the local vehicle will switch to the lane-changing mode. As shown in Fig.6, the picture in the left is the schematic diagram of lane-changing scenario, once the local vehicle crosses the red dotted line, it will switch to the lane-changing mode. The environment APF in this lane-changing mode is also presented in Fig.6. In this situation, the X-axis represents the position of the road in the longitudinal direction, and the Y-axis represents position of the road in lateral direction, in which $[-1.5, 1.5]$ is the right lane and $[1.5, 4.5]$ is the left lane. Besides, the bump in the right lane represents the obstacle vehicle, when the THW of the local vehicle reaches the preset value, the local vehicle will switch to the lane-changing mode. In this mode, the APF in adjacent lane is much lower than current lane, so the local vehicle will change lane along the direction of the APF downward. Fig.6 (a) represents the cautious style, while Fig.6 (b) represents the aggressive style. Under the cautious style, the THW of entering the lane-changing mode is longer than that of the aggressive style, and it also takes longer to change the lane.

As mentioned before, the difference among different driving style modes in lane-changing is the lane-changing duration. With this in mind, we adjust the cost function in lane-changing mode, which is shown as follows:

$$\begin{aligned} J_{lane\ change} &= (\xi(t), u(t-1), \Delta u(t)) \\ &= \sum_{i=1}^{N_p} \left\| U_{APFlane\ change}(t+i|t) \right\|_Q^2 \\ &\quad + \sum_{i=1}^{N_p} \| v(t+i|t) - v_{des} \|_R^2 \\ &\quad + \sum_{i=1}^{N_c} \| \Delta u(t+i|t) \|_S^2 \end{aligned} \tag{17}$$

where $U_{APFlane\_change}$ is defined as:

$$U_{APFlane\ change} = U_{road} + U_{goal} + U_{time} \tag{18}$$

where, U_{goal} is target APF, and U_{time} is lane-changing duration APF.

Environmental APF guides the vehicle to change lanes, and driving style APF determines the lane-changing duration. The other parts of the cost function are similar to Equation (12). At the end of each step, lane-changing safety judgment is introduced by calculating the vehicle APF of the predictive trajectory points. If the APF value is too large, there will be a risk of collision with the environment vehicle and the lane-changing should be abandoned. In this situation, the vehicle should decelerate to follow the front vehicle. After the lane-changing, the vehicle returns to free-flowing mode, and the triggering condition needs to be judged at each step. In addition, the criterion of the finishing lane-changing is that the vehicle crosses the lane line. The constraints are the same as those in the car-following mode, thus the optimal control problem of the trajectory planning considering driving styles under the lane-changing mode is:

$$\begin{aligned} &min_{\Delta u(t)} \left\{ J_{lane\ change} = (\xi(t), u(t-1), \Delta u(t)) \right\} \\ &\text{s. t. } \xi(k+1) = f(\xi(k), u(k)) \\ &\quad u(k) = u(k+1) + \Delta u(k) \\ &\quad u_{min}(k) \le u(k) \le u_{max}(k) \\ &\quad \Delta u_{min}(k) \le \Delta u(k) \le \Delta u_{max}(k) \end{aligned} \tag{19}$$

TABLE 1. Units for magnetic properties.

Parameter	Value	Unit
A_{road}	15	-
κ	0.01	-
ϕ	0.5	-
S_{min}	3	m
σ_{car}	0.5	-
A_{car}	15	-
A_{lane}	0.18	-
A_{thw}	1.4	-
A_{time}	1	-
N_p	25	-
N_c	2	-

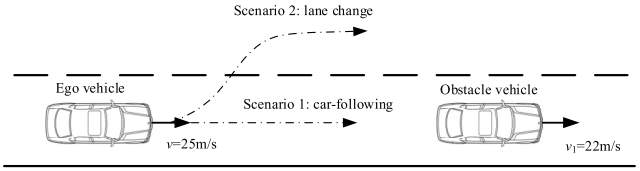

FIGURE 7. The scenarios definition.

TABLE 2. Computational efficiency of the algorithm.

Scenario	Time(s)/Step	Mean Time(s)
1	[0.11,0.22]	0.15
2	[0.14,0.31]	0.18

V. THE SIMULATION EXPERIMENT

The proposed trajectory planning and tracking approaches have been simulated by using MATLAB/Simulink and CarSim. Huang *et al.* [26] presented a control algorithm combining the APF approach with the MPC, but their method does not include driving styles. We also simulate their algorithm as a comparison, and the parameters used in the way are listed in the following Table 1.

A. TEST SCENARIO

The first scenario is used to verify the trajectory planning and tracking method considering the driving style in the car-following mode. The second scenario is used to verify the trajectory planning and tracking method in the lane-changing mode. The specific settings are as follows:

Scenario 1 is a car-following scenario. The road consists of two lanes, and there are two vehicles in the same lane. The distance between the two vehicles is 100 meters. The environment vehicle is in front of the local vehicle, and the speeds of the local vehicle and environment vehicle are 25m/s and 22m/s respectively. The local vehicle is in the car-following mode. Scenario 1 is set up as shown in the Fig. 7.

Scenario 2 is a simple lane-changing scenario. In this scenario, the local vehicle is in lane-changing mode, and the distance between the two vehicles is 80 meters. Additionally, the speeds of the ego vehicle and environment vehicle are 25m/s and 22m/s respectively.

B. THE SIMULATION RESULTS

The simulation run on the joint simulation platform of Carsim-Simulink, in which the Carsim is used as high-fidelity vehicle model. The *fmincon* function in Matlab is chose as solver. The PC used for simulation experiments is Intel(R) i9-9900 CPU, RAM 16G. The computational efficiency is shown in Table 2. The mean times per step for scenario 1 and 2 are 0.15s and 0.18s. In algorithm, we set the simulation step as 0.02s. Therefore, the algorithm cannot meet the requirement of real-time computational efficiency, which is the shortcoming for many MPC controllers [35]. Therefore, the algorithm proposed in this study can not be put into application of real autonomous. And we will improve this algorithm in future so that it can run in real-time.

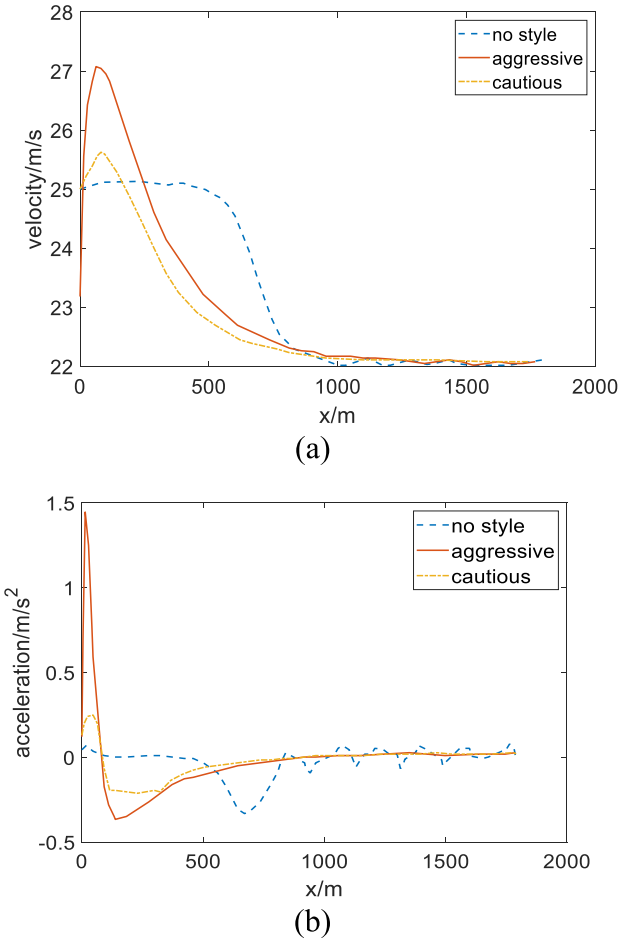

FIGURE 8. Scenario 1. (a) Speed curves under the two driving styles and no driving style (b) Longitudinal accelerations of the local vehicle under the two driving styles and no driving style.

Car-Following Scenario: Fig. 8(a) shows the speed curves for the two driving styles and no driving style. The simulation results of no driving style come from the method of a previous study [26]. As seen below, the red line indicates the speed obtained under the aggressive driving style, the yellow line shows that of the cautious driving style, and the blue line is the result of no driving style. At the beginning, there will be a short period of acceleration due to goal APF. With the continuous action of the time headway APF, the speed of the vehicle will gradually approach the front vehicle. Finally, the speed of the local car will be the same as that of the car in front, then

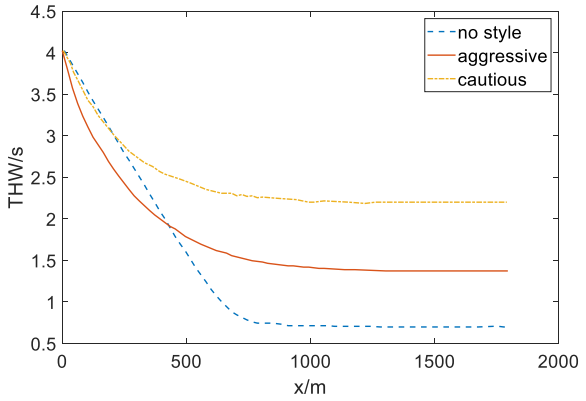

FIGURE 9. Time headway of the local vehicle under the two driving styles and no driving style.

the former changes to a stable car-following state. The speed dropping begins earlier in the cautious driving mode. This is because its THW is large. And the speed dropping rate of the aggressive driving mode is significantly larger than that of the cautious driving mode. Under no driving style, the local vehicle will contain 25m/s at first. When it gets close enough to the car in front, the obstacle potential field forces it to slow down and reach the same speed as the car in front.

Fig. 8(b) shows the longitudinal accelerations under the two driving styles and no driving style, and the accelerations are all within the limits of constraints. In addition to this, the range of the acceleration in the aggressive driving mode is obviously greater than that in the cautious driving mode. Under no driving style, the acceleration of the car will be up and down frequently.

The THW of the local vehicle under the two driving styles is shown in Fig. 9. The THW can reflect the differences in trajectory planning between the two driving style modes. Because the speed of the local vehicle is greater than its preceding vehicle, the THW is decreased continuously and finally reaches an expected value. We can see the THW of the aggressive driving mode dropping faster than the cautious driving mode. The final THW in the cautious driving mode reaches about 1.76 seconds, while it is at about 1.15 seconds in the aggressive driving mode, which conforms to the expectation. Under no driving style, the final THW of the local vehicle is related to the APF of the vehicle in front.

Lane-Changing Scenario: The trajectories under the two driving styles and no driving style are shown in Fig.10 (a). It can be seen from the figure that the lane-changing of the aggressive driving starts at about 190m. Furthermore, it is not easy to observe the lane-changing duration in Fig. 10(a). In order to intuitively analyze the difference in lane-changing duration between the two driving styles, we transform Fig. 10(1) to Fig. 10(b). In this scenario, the speed of the two styles of vehicles is stable at 25m/s, so we can calculate the lane-changing time through the lane-changing distance. The lane-changing distance of aggressive driving style is about 42 m, and the lane-changing duration is about 1.7 s, which is in line with the previous setting. Similarly,

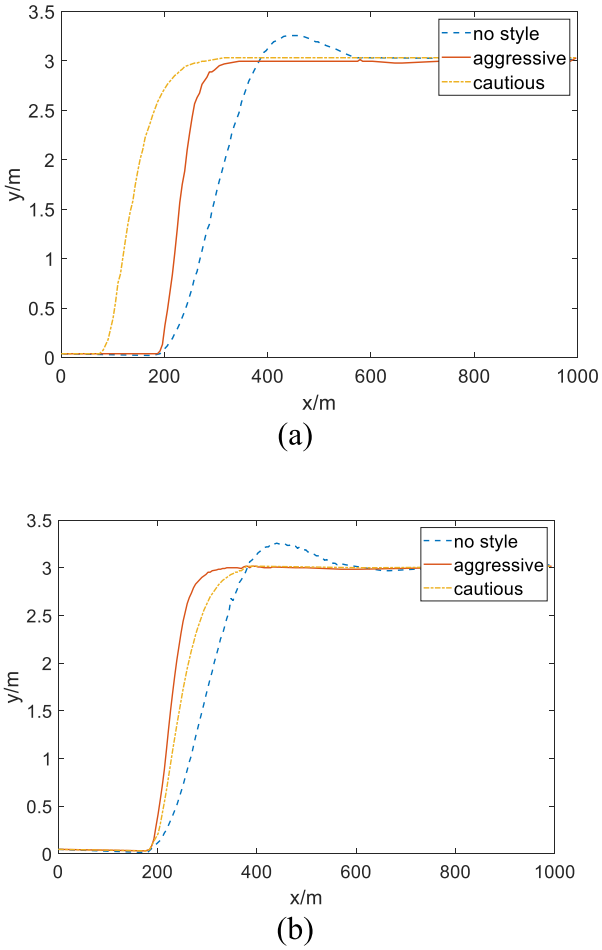

FIGURE 10. Scenario 2. (a) Trajectories of the local vehicle planed under the two driving styles and no driving style. (b) Trajectories adjusted.

as for cautious driving, the lane-changing distance is about 62 m, and the lane-changing duration under cautious driving style mode is about 2.5s, which meets the requirements of the current driving style mode. Under no driving style, the timing of lane-changing is similar to that of the aggressive style, but the duration of lane-change is longer than those in the two driving styles.

Fig. 11(a) shows the longitudinal accelerations under the two driving styles and no driving style. It can be noted that the accelerations are both within the limits of constraints, and the acceleration in the aggressive driving mode is obviously greater than that in the cautious driving mode. Fig. 11(b) shows the local vehicle heading angle under the two driving styles and no driving style. As seen in the figure, the time when the heading angle begins to change is when the lane-changing begins. The turning angle amplitude of aggressive mode is greater than that of cautious mode, which is also in line with our expectations.

Fig. 12 shows the corresponding THW at lane-changing state under the two driving styles and no driving style. In the aggressive mode, the local car changes lanes when THW is 1.15s, and in the cautious mode, the local car changes lanes when THW is 1.76s, which is exactly what we expected.

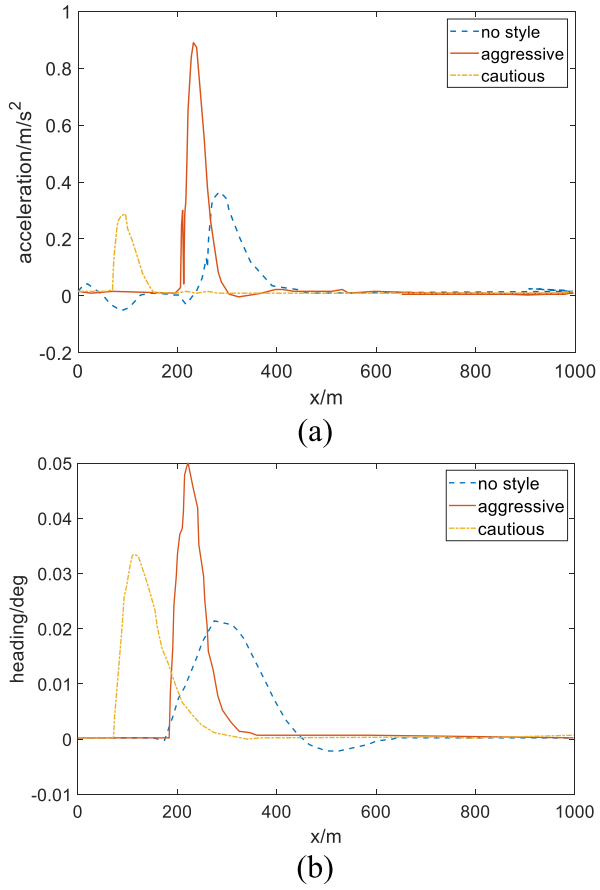

FIGURE 11. Scenario 2. (a) Longitudinal accelerations of the local vehicle under the two driving styles and no driving style. (b) Heading angle under the two driving styles and no driving style.

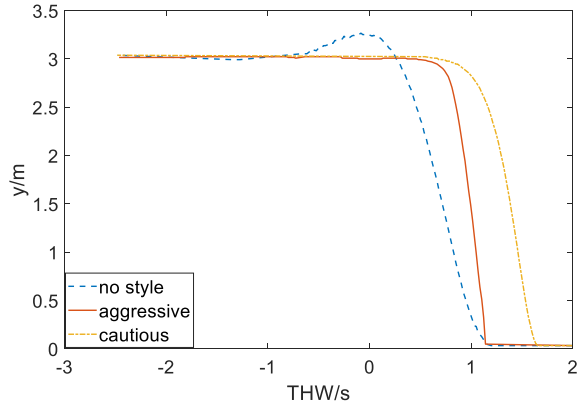

FIGURE 12. The corresponding THW at lane-change state under the two driving styles and no driving style.

Based on the results above, we can conclude that the local car can reflect its own style in different driving modes. Under no driving style, when the local vehicle changes the lane, its THW is similar to that of the aggressive style, but the duration of lane-changing is longer than those in the two driving styles.

VI. CONCLUSION

In this paper, a trajectory planning and tracking control method of autonomous vehicles considering driving styles has been proposed. A novel APF model is established, which is made up of environmental APF and driving style APF. Specifically, the environmental APF is adopted for obstacle avoidance, while driving style APF is employed to generate the planned trajectory, which conforms to human drivers' different driving styles. The controller can plan a trajectory and track it by adding the APF to the cost function of the MPC. Therefore, the occupants of autonomous vehicles can select different driving style modes, i.e., aggressive driving mode and cautious driving mode. The result shows that the planned trajectory can conform to the selected driving style when the driving mode is selected. Compared with the result of no driving style, the method in this study is more stable and is in line with people's habits.

REFERENCES

[1] J. Liu, W. Han, C. Liu, and H. Peng, "A new method for the optimal control problem of path planning for unmanned ground systems," *IEEE Access*, vol. 6, pp. 33251–33260, 2018.
[2] M. Kuderer, S. Gulati, and W. Burgard, "Learning driving styles for autonomous vehicles from demonstration," in *Proc. IEEE Int. Conf. Robot. Autom. (ICRA)*, Seattle, WA, USA, May 2015, pp. 2641–2646.
[3] N. Lin, C. Zong, M. Tomizuka, P. Song, Z. Zhang, and G. Li, "An overview on study of identification of driver behavior characteristics for automotive control," *Math. Problems Eng.*, vol. 2014, pp. 1–15, Mar. 2014.
[4] Z. Chen, Y. Zhang, C. Wu, and B. Ran, "Understanding individualization driving states via latent Dirichlet allocation model," *IEEE Intell. Transp. Syst. Mag.*, vol. 11, no. 2, pp. 41–53, Summer 2019.
[5] G. Li, W. Lai, X. Sui, X. Li, X. Qu, T. Zhang, and Y. Li, "Influence of traffic congestion on driver behavior in post-congestion driving," *Accident Anal. Prevention*, vol. 141, Jun. 2020, Art. no. 105508.
[6] G. Li, S. E. Li, B. Cheng, and P. Green, "Estimation of driving style in naturalistic highway traffic using maneuver transition probabilities," *Transp. Res. C, Emerg. Technol.*, vol. 74, pp. 113–125, Jan. 2017.
[7] D. Yi, J. Su, L. Hu, C. Liu, M. Quddus, M. Dianati, and W.-H. Chen, "Implicit personalization in driving assistance: State-of-the-art and open issues," *IEEE Trans. Intell. Vehicles*, vol. 5, no. 3, pp. 397–413, Sep. 2020.
[8] S. Lefevre, A. Carvalho, and F. Borrelli, "A learning-based framework for velocity control in autonomous driving," *IEEE Trans. Autom. Sci. Eng.*, vol. 13, no. 1, pp. 32–42, Jan. 2016.
[9] M. Hasenjager and H. Wersing, "Personalization in advanced driver assistance systems and autonomous vehicles: A review," in *Proc. IEEE 20th Int. Conf. Intell. Transp. Syst. (ITSC)*, Yokohama, Japan, Oct. 2017, pp. 1–7.
[10] Y. Xing, C. Lv, D. Cao, and C. Lu, "Energy oriented driving behavior analysis and personalized prediction of vehicle states with joint time series modeling," *Appl. Energy*, vol. 261, Mar. 2020, Art. no. 114471.
[11] Y. Xing, C. Lv, and D. Cao, "Personalized vehicle trajectory prediction based on joint time-series modeling for connected vehicles," *IEEE Trans. Veh. Technol.*, vol. 69, no. 2, pp. 1341–1352, Feb. 2020.
[12] O. Khatib, "Real-time obstacle avoidance for manipulators and mobile robots," in *Proc. IEEE Int. Conf. Robot. Autom.*, St. Louis, MO, USA, Mar. 2003, pp. 90–98.
[13] Y. Huang, H. Ding, Y. Zhang, H. Wang, D. Cao, N. Xu, and C. Hu, "A motion planning and tracking framework for autonomous vehicles based on artificial potential field elaborated resistance network approach," *IEEE Trans. Ind. Electron.*, vol. 67, no. 2, pp. 1376–1386, Feb. 2020.
[14] P. Wang, S. Gao, and L. Li, "Obstacle avoidance path planning design for autonomous driving vehicles based on an improved artificial potential field algorithm," *Energies*, vol. 12, no. 12, pp. 23–42, Jun. 2019.
[15] H. Guo, D. Cao, H. Chen, Z. Sun, and Y. Hu, "Model predictive path following control for autonomous cars considering a measurable disturbance: Implementation, testing, and verification," *Mech. Syst. Signal Process.*, vol. 118, pp. 41–60, Mar. 2019.
[16] C. Zhang, D. Chu, S. Liu, Z. Deng, C. Wu, and X. Su, "Trajectory planning and tracking for autonomous vehicle based on state lattice and model predictive control," *IEEE Intell. Transp. Syst. Mag.*, vol. 11, no. 2, pp. 29–40, Mar. 2019.
[17] S. Li, Z. Li, Z. Yu, B. Zhang, and N. Zhang, "Dynamic trajectory planning and tracking for autonomous vehicle with obstacle avoidance based on model predictive control," *IEEE Access*, vol. 7, pp. 132074–132086, 2019.

[18] K. Berntorp, R. Quirynen, and S. Di Cairano, "Steering of autonomous vehicles based on friction-adaptive nonlinear model-predictive control," in *Proc. Amer. Control Conf. (ACC)*, Philadelphia, PA, USA, Jul. 2019, pp. 965–970.
[19] S. Velhal and S. Thomas, "Improved LTVMPC design for steering control of autonomous vehicle," *J. Phys. Conf. Ser.*, vol. 783, no. 1, pp. 12–28, Jan. 2017.
[20] X. Du, K. K. K. Htet, and K. K. Tan, "Development of a genetic-algorithm-based nonlinear model predictive control scheme on velocity and steering of autonomous vehicles," *IEEE Trans. Ind. Electron.*, vol. 63, no. 11, pp. 6970–6977, Nov. 2016.
[21] M. A. Abbas, R. Milman, and J. M. Eklund, "Obstacle avoidance in real time with nonlinear model predictive control of autonomous vehicles," *Can. J. Elect. Comput. Eng.*, vol. 40, no. 1, pp. 12–22, May 2017.
[22] R. Soloperto, J. Kohler, F. Allguwer, and M. A. Müller, "Collision avoidance for uncertain nonlinear systems with moving obstacles using robust model predictive control," in *Proc. 18th Eur. Control Conf. (ECC)*, Naples, Italy, Jun. 2019, pp. 811–817.
[23] Z. Wang, G. Li, H. Jiang, Q. Chen, and H. Zhang, "Collision-free navigation of autonomous vehicles using convex quadratic programming-based model predictive control," *IEEE/ASME Trans. Mechatronics*, vol. 23, no. 3, pp. 1103–1113, Jun. 2018.
[24] Z. Huang, Q. Wu, J. Ma, and S. Fan, "An APF and MPC combined collaborative driving controller using vehicular communication technologies," *Chaos, Solitons Fractals*, vol. 89, pp. 232–242, Aug. 2016.
[25] Y. Rasekhipour, A. Khajepour, S.-K. Chen, and B. Litkouhi, "A potential field-based model predictive path-planning controller for autonomous road vehicles," *IEEE Trans. Intell. Transp. Syst.*, vol. 18, no. 5, pp. 1255–1267, May 2017.
[26] Z. Huang, D. Chu, C. Wu, and Y. He, "Path planning and cooperative control for automated vehicle platoon using hybrid automata," *IEEE Trans. Intell. Transp. Syst.*, vol. 20, no. 3, pp. 959–974, Mar. 2019.
[27] W. Wang, J. Xi, and D. Zhao, "Driving style analysis using primitive driving patterns with Bayesian nonparametric approaches," *IEEE Trans. Intell. Transp. Syst.*, vol. 20, no. 8, pp. 2986–2998, Aug. 2019.
[28] J. Wang, R. Chi, L. Zhang, K. Li, and T. Yu, "Study on forward collision warning-avoidance algorithm based on driver characteristics adaptation," *J. Highway Transp. Res. Develop.*, vol. 26, no. 1, pp. 7–12, Dec. 2009.
[29] B. Zhu, Y. Jiang, J. Zhao, R. He, N. Bian, and W. Deng, "Typical-driving-style-oriented personalized adaptive cruise control design based on human driving data," *Transp. Res. C, Emerg. Technol.*, vol. 100, pp. 274–288, Mar. 2019.
[30] Y. Chen, C. Hu, and J. Wang, "Motion planning with velocity prediction and composite nonlinear feedback tracking control for lane-change strategy of autonomous vehicles," *IEEE Trans. Intell. Vehicles*, vol. 5, no. 1, pp. 63–74, Mar. 2020.
[31] M. Vechione, E. Balal, and R. L. Cheu, "Comparisons of mandatory and discretionary lane changing behavior on freeways," *Int. J. Transp. Sci. Technol.*, vol. 7, no. 2, pp. 124–136, Jun. 2018.
[32] X. Li, W. Wang, and M. Roetting, "Estimating Driver's lane-change intent considering driving style and contextual traffic," *IEEE Trans. Intell. Transp. Syst.*, vol. 20, no. 9, pp. 3258–3271, Sep. 2019.
[33] A. Doshi and M. M. Trivedi, "Examining the impact of driving style on the predictability and responsiveness of the driver: Real-world and simulator analysis," in *Proc. IEEE Intell. Vehicles Symp.*, San Diego, CA, USA, Jun. 2010, pp. 232–237.
[34] M. T. Wolf and J. W. Burdick, "Artificial potential functions for highway driving with collision avoidance," in *Proc. IEEE Int. Conf. Robot. Autom.*, Pasadena, CA, USA, May 2008, pp. 3731–3736.
[35] J. Liu, W. Han, Y. Zhang, Z. Chen, and H. Peng, "Design of an online nonlinear optimal tracking control method for unmanned ground systems," *IEEE Access*, vol. 6, pp. 65429–65438, 2018.

HAORAN LI (Student Member, IEEE) received the B.E. and M.S. degrees in vehicle engineering from the Wuhan University of Technology, Wuhan, China, in 2011 and 2014, respectively, where he is currently pursuing the Ph.D. degree with the Transportation Systems Research Center, focusing on the research of automated and connected vehicle.

CHAOZHONG WU received the B.E. degree in marine engineering, the M.S. degree in management science and engineering, and the Ph.D. degree in transportation engineering from the Wuhan University of Technology, Wuhan, China, in 1996, 1999, and 2002, respectively. He was a Visiting Scholar with the University of Regina, Canada, and Northeastern University, USA, in 2006 and 2015, respectively. He is currently a Professor and the Director of the Intelligent Transportation Systems Research Center, Wuhan University of Technology. He is an expert in traffic safety, connected vehicle, and intelligent transportation systems. He has published over 60 journal articles and holds 11 patents. He was a recipient of the New Century Excellent Talent of Ministry of Education, China, in 2010, the Young Talent of Ministry of Transport, China, in 2012, the Distinguished Young Scholar of Hubei Province of China, in 2012, and the Young Leading Talent of Ministry of Transport, China, in 2014. He serves as an associate editor for some journals.

DUANFENG CHU (Member, IEEE) received the B.E. and Ph.D. degrees in mechanical engineering from the Wuhan University of Technology, Wuhan, China, in 2005 and 2010, respectively. He is currently a Professor with the Intelligent Transportation Systems Research Center, Wuhan University of Technology, focusing on the research of automated and connected vehicle, and intelligent transportation systems. He has visited the University of California, Berkeley, CA, USA, and The Ohio State University, Columbus, OH, USA, in 2009 and 2017, respectively. He has been a reviewer for several international journals and conferences in the field of automated vehicle.

LIPING LU received the B.E. degree in industry automation from the Hubei University of Technology, Wuhan, China, in 1999, the M.S. degree in automation theory and engineering from the Wuhan University of Technology, Wuhan, in 2002, and the Ph.D. degree in computer science (obtained Sino-French Doctoral scholarships) from the Institut National Polytechique de Lorraine (INPL), Nancy, France, and the Wuhan University of Technology, in 2006. She is currently an Associate Professor with the College of Computer Science and Technology, Wuhan University of Technology. Her research interests include vehicle networking, computational simulation, and embedded systems. She was a Visiting Scholar with The Ohio State University, Columbus, OH, USA, in 2019.

KEN CHENG received the B.E. degree in mechanical engineering from Huazhong Agricultural University, Wuhan, China, in 2017. He is currently pursuing the master's degree in computer technology with the Wuhan University of Technology, Wuhan. His research interests include reinforcement learning and decision-making.